Discover Sustainability

Research

Modelling and analysis of strength and durability properties of internal curing concrete using PEG 400 and artificial neural network

Sowjanya Gowdra Virupakshappa[1] · Anadinni Shrishail Basappa[2] · Mahadevaiah Thimmarayappa[3] · Channa Keshava Naik Narayana[4] · Abdulrajak Buradi[5] · Addisu Frinjo Emma[6]

Received: 22 January 2024 / Accepted: 1 April 2024
Published online: 29 April 2024

Abstract
The traditional curing processes necessitate a large amount of water. This is especially difficult in locations where there is a lack of water and for construction of high-rise structures. In this research article, we provide a remedy by inventing concrete that will not require additional water for curing. In the present work, polyethylene glycol was utilized as an internal curing agent in varying percentages. The internally cured concrete with polyethylene glycol was cured at ambient conditions, whereas the conventional concrete without polyethylene glycol was kept in water for curing. Fresh and hardened characteristics of concrete with and without polyethylene glycol are compared. The results revealed that 1.5% polyethylene glycol is an optimum percentage where maximum strength and durable properties are achieved. The microstructure of internal curing concrete indicates that the pore sizes are small compared to conventional concrete. The crystallite size is smaller in internal curing compared to conventional concrete mixtures, resulting in an acceleration of the hydration process in concrete with smaller crystallites.Further experimental results are compared with ANN. Predicted results are very close to experimental values.

Keywords Internal curing · Artificial neural network · Polyethylene glycol · Compressive strength · Durability

1 Introduction

Water is our lifeline; preserving water for future generations is essential. Water is used in every stage of construction; a large quantity of water is mainly utilized for curing [1]. Curing is the procedure used to encourage the cement hydration process. It includes controlling temperature and moisture movement from and into the concrete [2]. Proper curing is not done if the member is vertical, in places with scanty water, human negligence, or difficult terrain [3]. Improperly cured structural elements fail to attain strength and durability criteria.

✉ Addisu Frinjo Emma, addisuf@du.edu.et; Sowjanya Gowdra Virupakshappa, gvsowju@gmail.com; Anadinni Shrishail Basappa, anadinnisb@gmail.com; Mahadevaiah Thimmarayappa, mahadevaiaht@gmail.com; Channa Keshava Naik Narayana, naikphd.sit@gmail.com; Abdulrajak Buradi, arbnitk@gmail.com | [1]Department of Civil Engineering, Sri Siddhartha Institute of Technology, SSAHE, Tumkur 572105, India. [2]Department of Civil Engineering, School of Engineering, Presidency University, Bengalore 560064, India. [3]Department of Civil Engineering, BGS Institute of Technology, Adichunchanagiri University, B G Nagar 571448, Karnataka, India. [4]Department of Mechanical Engineering, BGS Institute of Technology, Adichunchanagiri University, B G Nagar 571448, Karnataka, India. [5]Department of Mechanical Engineering, Nitte Meenakshi Institute of Technology, Bangalore, Karnataka 560064, India. [6]Southern Ethiopia Region, College of Engineering and Technolgy, School of Mechanical and Automotive Engineering, Dilla University, 419, Dilla, Ethiopia.

Water can be saved by using internal curing concrete. External curing is done after mixing, placing and finishing in a conventional method of curing [4]. In contrast, internal curing provides additional moisture, which is not a part of mixing water. It enhances hydration and minimizes self-desiccation and shrinkage [5–7]. Compared to traditional curing, the strength of internally cured concrete is higher. Evaporation reduces the surface tension of water in the concrete, reducing the concrete's water maintenance limit for nonstop hydration [8].

Concrete can be internally cured in two different ways [9, 10]

1. By using self-curing chemicals [12, 45]: These chemicals will minimize the evaporation of water from the concrete surface and help in water retention. Ex: Poly Ethylene Glycol and Super Absorbent Polymer.
2. By using porous presoaked lightweight aggregates [40, 46]: These aggregates are presoaked before being used to provide an internal water source. It increases the hydration process and decreases autogenous shrinkage. Ex: pumic stone, fly ash aggregates, expanded shale.

Internal curing helps improve performance in concrete mixtures with a higher W/C when the curing conditions are poor [14]. Several researchers utilized polymers soluble in water as self-curing agents. Internal curing agents such as polyacrylamide and polyethylene-glycol have been proven to be very efficient at retaining water in concrete and thus providing adequate water for cement [15].

ANN is an abbreviation for "Artificial Neural Network." It is a computer model inspired by the form and operation of neural networks in the human brain. ANNs are used in machine learning [41] and artificial intelligence to address complicated issues that standard algorithms cannot handle [38]. An artificial neural network is made up of linked nodes called neurons or units that are organized into layers [39]. An ANN is a computer model whose architecture closely resembles how the human brain acquires knowledge [13]. It consists of a network of interconnected processing components known as neurons. The neurons are organized rationally into two or more layers and communicate with one another through weighted connections [11]. These scalar weights determine the nature and strength of the impact between the linked neurons. Neural networks are dense, parallel, interconnected networks with many simple processes termed nodes, units, or neurons. Synapses are the connections between the neurons.

1.1 Hydration mechanism in traditional concrete

The hydration reactions start immediately when water is poured into regular Portland cement (OPC) powder. This string of chemical processes causes the cement paste to solidify and harden. Calcium sulfoaluminate hydrate needle-like crystals, particularly ettringite, form quickly. Ettringite eventually converts into monosulfate hydrate [47]. The voids that were originally occupied by water and hydrated cement particles are filled by massive prismatic crystals of calcium hydroxide and minute calcium silicate hydrates (C-S-H) 2 h after the cementation procedure starts (as indicated in Eqs. (1), (2), (3), (4), (5), (6) hydration product, which accounts for roughly 60% of the volume of solids, is calcium silicate hydrate. It comprises a layer of massively surface-areas sponge-like structures (500 m^2/g). The creation of C-S-H and van der Waals physical adhesion forces are mainly responsible for the product's ultimate strength. The second most common substance, calcium hydroxide, accounts for around twenty-five per cent of the whole. It has a reduced surface area and comprises big plate-like crystals instead of C-S–H [47, 48]. Because it is soluble in compared to C-S–H and reduces van der Waal forces, concrete is more reactive to acidic solutions. Nearly fifteen per cent of the solid volume of calcium sulfoaluminate contributes to the cementitious structure's characteristics. Due to the presence of mono-sulfate hydrate, the chemical resistance of the cementitious end product against sulphate attack is a problem. Figure 1 illustrates electron microscopic representations of a hardened hydrated cement mixture.

$$2Ca_3SiO_3 + 7H_2O \leftrightarrow Ca_3SiO_3(OH)_8 + 3Ca(OH)_2 \quad (1)$$

$$2Ca_2SiO_4 + 5H_2O \leftrightarrow Ca_3Si_2O_3(OH)_8 + 3Ca(OH)_2 \quad (2)$$

$$Ca_4Al_2Fe_2O_{10} + 7H_2O \leftrightarrow Fe_2O_3 + Ca3Al_2(OH)_{12} + Ca(OH)_2 \quad (3)$$

$$CaO + H_2O \leftrightarrow Ca(OH)_2 \quad (4)$$

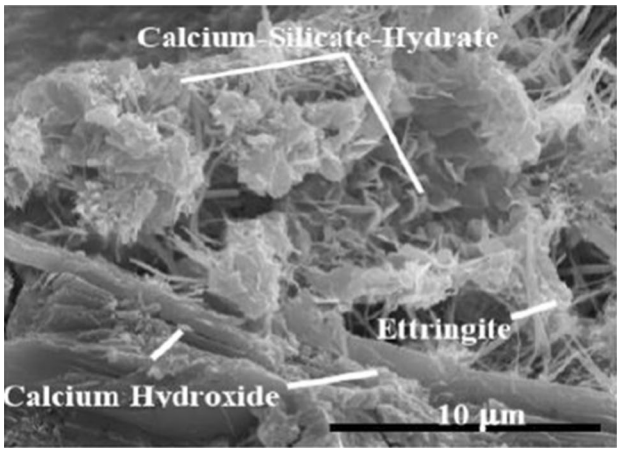

Fig. 1 Electron microscopic images of hardened cement after hydration [49]

$$Ca_3Al_2O_6 + 3CaSO_4 2H_2O + 26\,H_2O \leftrightarrow \left[Ca_3Al(OH)_6 \cdot 12H_2O\right]_2\left(SO_4\right) \cdot 32H_2O \tag{5}$$

$$\left[Ca_3Al(OH)_6 \cdot 12H_2O\right]2 \cdot \left(SO_4\right)_3 \cdot 2H_2O + Ca_3Al_2O_6 + 4H_2O \leftrightarrow 3\left[Ca_2Al(OH)_6 \cdot 2H_2O\right]2SO_4 \cdot 2H_2O \tag{6}$$

1.2 Polyethylene glycol

Polyethylene-glycol is a condensing polymer made of ethylene oxide and water, having formula. H $(OCH_2CH_2)_n$ OH where n represents the average number of repeating groups of ox ethylene, typically between 4 and around 180 [50]. It is obvious that theoretically, by adding additives, the vapour pressure of water will decrease, thereby reducing the evaporation rate above the concrete surface. Raoult's Law states that when the vapour pressure of the solute in the pure condition is lesser than the vapour pressure of the solvent in the pure condition [50–54]. Because of this, it was found that using water-soluble polymers in concrete like PEG as self-curing is both efficient and effective in retaining water and improving the process of hydration [52, 55, 56]. Additionally, polymeric chains made of hydrophilic units create hydrogen bonds with water molecules. A weak link between hydrogen and strongly electronegative atoms in other molecules is known as a hydrogen bond [50]. As seen in Fig. 2, the electrostatic attraction between the hydrogen atom and the electronegative atom results from a positive charge at the hydrogen atom. To minimize the effects of self-desiccation in concrete, water-soluble polymers having either hydroxyl (-OH-) or ether (-O-) functional groups have been employed

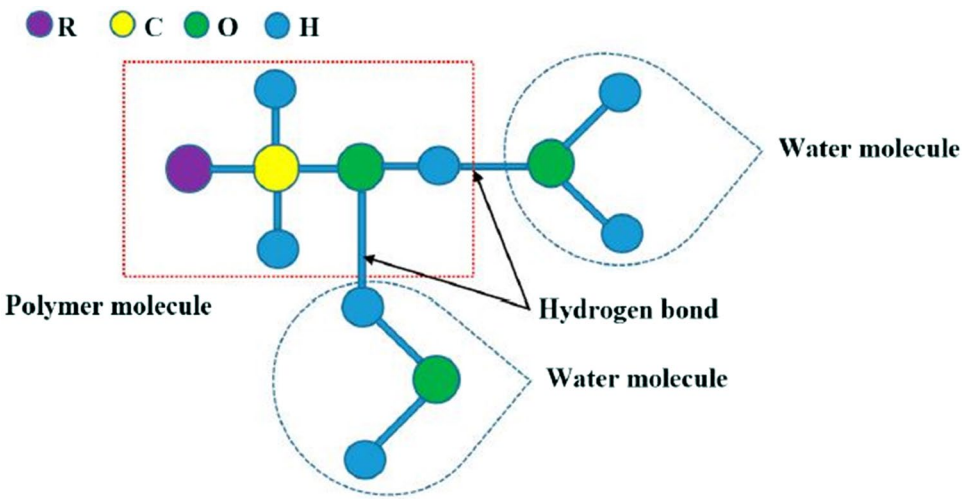

Fig. 2 Hydrogen bonds between molecules of water and an –OH group on a polymer molecule

as the chemical [50, 57]. Using PEG as an internal curing agent, previous studies determined concrete's durability, water retention, hydration, compressive strength, and microstructure characteristics [53, 54, 56–58].

2 Literature review

2.1 Literature review on internal curing

Akhib K. MD et al. [16] determined the mechanical properties of M65 concrete. In this paper, he replaced cement with fly ash and used PEG as a self-curing agent. It is observed maximum strengths are gained at a 1% dosage of PEG400.

Bottom ash was taken as an self curing agent, and the compression strength of the concrete was improved [17]. Prakash Mandiwal et al. [18] did experiments on M20 and M25 by replacing cement with PEG 400 in varying percentages (0%. 0.8%, 1.5%, 2.4% and 3.2%) to evaluate strength properties. Maximum strength was achieved at 2.4% and 1.6% for M20 and M25 concrete, respectively. Sebastin S [19] studied the properties of internally cured concrete by replacing fine aggregate with granite powder and adding 0.5% of the super absorbent polymer as a curing agent. The experimental results revealed that the strength was improved in self-curing concrete compared to ordinary concrete.

Sastry and Kumar [20] evaluated the performances of various polymers and found that polyethylene glycol is more efficient than the others. Zhong et al. [21] studied different superabsorbent groups like cationic, anionic and non-ionic groups. The study revealed cationic and anionic superabsorbent groups are considered excellent self-curing agents. Quin [22] explored the particle size effect of superabsorbent polymer on the movement of water behaviour. The superabsorbent polymer with reduced particle size was shown to provide water for hydration for a longer period.

It is suggested that 50% recycled aggregates be used for interior curing since this will improve performance and provide well-known sustainability benefits [23]. Balapour et al. [24] investigated the feasibility of bottom coal ash for self-curing concrete & discovered that the bottom ash might release eighty-five per cent water at ninety-four per cent relative humidity. The super-absorbed polymer used as a self-curing agent was very efficient in controlling the shrinkage of CSH with low w/c mortar [25]. Doha et al. [26] applied the self-curing concept to high-performance concrete. They concluded that it effectively increases strength properties by providing a dense and compacted interfacial transition zone. Shivaprasad et al. [27] experimented to determine strength characteristics of fibre-reinforced concrete using PEG400 and CURE WB as self-curing agents. Metakaolin (10%) and flyash(30%) replace cement here. Steel fibre percentage (0.5%, 0.75% and 1%). Results revealed that PEG 400 is more efficient. Xiao Yuan [28] compared traditional curing and self-curing by preparing cubes and cylinders for M10, M20 and M30 concrete. The finding showed that self-curing concrete performed better than traditional concrete. The experiment was conducted on M30 internal curing concrete by incorporating wood powder and PEG as curing agents in varied percentages. It showed that maximum strength is gained at 6% of wood powder and 1.55 of PEG 400 [29].

2.2 Literature review on ANN

Jose Manuel Palomino Ojeda et al. [30] proposed 5 ANNs to find the compression strength of concrete @ 7, 14 and 28 days. The network consisted of five inputs, two hidden and one output layer (compressive strength). Results revealed ANN can be treated as a non-destructive option for quality control in the construction sector. This method is effective and valid for evaluating the compression strength of concrete.

An ANN for compression strength prediction was developed by Saha et al. [31, 44]. For predicting the properties, this ANN model used eight input parameters. There was a perfect correlation between the experimental and predicted compression strength values. Compared with the multivariable regression technique, the ANN model gave a very low MSE and high efficiency. Reddy [32, 42, 43] used feed-forward ANN to assess the strength property of concrete. The model produced an RMSE of 0.046 and a MAPE of 0.0348. The predicted values from the ANN closely matched the outcomes of the experiment. The tensile compression strength of concrete was estimated by developing ANN and the modified firefly algorithm. The created model improved property prediction accuracy and was faster than previous methods by Bui et al. [33]. Awoyera [34] utilized the Levenberg–Marquardt (LM) of MFBP–ANN to determine strength properties. With a confidence level of 99 per cent, the created ANN model accurately predicted the tested strength properties. Kalpan et al. [35] adopted feed-forward ANN with backpropagation to estimate concrete compression strength for different types of concrete, water absorbed, curing conditions, w/c, curing duration and penetration. The suggested method uses the material's qualities to provide a non-destructive method for determining compressive strength. Hunga P D et al. [36]

studied damaged concrete surface classification by developing a deep convolution neural network. The accuracy of the result was found to be 93% and 95% on the test and training set, respectively. Elinwa Augustine Uchechukwu's [37] neural networks were developed to determine the effects of incorporating palm kernel shells as aggregates on concrete compressive strength. This study used an ANN with a 6 factor input neuron, 2 hidden layers of 18 and 12 factors each, and 1 output neuron for compressive strength. The parameter estimations (ANN and Statistics) are within the 95 per cent confidence limits and very significant ($P < 0.05$).

Traditional concrete curing procedures use water, which poses problems in water-stressed areas and high-rise building scenarios. Furthermore, traditional curing procedures may not completely capitalize on the potential for improving concrete qualities. This study investigates the feasibility and usefulness of employing Polyethylene Glycol (PEG-400) as an internal curing agent for concrete. The main issue is establishing how internal curing using PEG-400 might increase the strength and durability attributes of concrete while minimizing water demand and environmental effects.

The research objectives are designed to address the problem formulation and contribute to advancing concrete technology and construction practices. The study seeks to achieve the following objectives:

- Examine the effect of varying concentrations of PEG-400 on the strength and durability properties of concrete subjected to internal curing. Determine the optimal PEG-400 concentration for achieving the highest mechanical performance and improved durability.
- Compare the mechanical properties of internally cured concrete with PEG-400 to those of conventionally cured concrete. Assess how internal curing improves strength, split tension, and flexure properties while mitigating water absorption.
- Investigate the microstructural changes induced by internal curing with PEG-400. Analyze how the presence of PEG-400 affects the pore sizes and distribution compared to traditional curing methods.
- Utilize an ANN to model the relationship between PEG-400 concentration, curing conditions, and concrete properties. Train the ANN to predict concrete properties based on input parameters and compare the predicted values with experimental results.
- Evaluate the sustainability and practical applicability of internal curing with PEG-400 in various construction scenarios. Consider the reduction in water demand, potential environmental benefits, and the feasibility of implementing the proposed technique in real-world construction projects.

The research is relevant in the fields of concrete technology and construction engineering. The research presents a unique way to improve concrete strength and durability by internal curing utilizing PEG-400 by addressing the issue of water shortage and the obstacles faced by existing concrete curing methods. The data show that this strategy decreases water usage and improves mechanical qualities, including compression, split tension, and flexure strength, while reducing water absorption and sorptivity. The study provides a sustainable alternative to standard curing practices, particularly in areas where water is scarce, and high-rise development necessitates efficient curing processes.

3 Materials and methodology

In this work, concrete of M40 grade has been considered, whose target strength was 48.25 N/mm^2 as per the Indian standard code (IS 10262–2019). OPC 43 grade was utilized for the preparation of concrete. About 15% of cement is replaced by fly ash. The specific gravity of cement and fly ash was 3.10 and 2.09 (IS 4031-Part I, 1998), respectively. Crushed stone sand is used as fine aggregates with a fineness modulus of 3.78 and a specific gravity of 2.56 (IS 2386-Part III: 1963), and 20 mm size crushed aggregate has been used as coarse aggregate with a specific gravity of 2.66. The water absorption values for fine aggregates and coarse aggregates were found to be 1.18% and 0.48%, respectively. Portable water is used for casting. New generation admixture Master Glenium SKY 8233 based on modified polycarboxylic ether is adopted; relative Density is 1.08 + 0.01 @25 °C. Internal curing agent Poly ethylene glycol-400 is used. The chemical formula is 2nH4n + 2On + 1. Density is 128 g/cm^3, and the melting point is 4 to 8 °C (39 to 460F; 277 to 281 K). The specific gravity of PEG 400 is 1.124.

Fresh M40 grades concrete was prepared for different proportions of self-curing agents (0.5%, 1%, 1.5% and 2%). Workability was determined by conducting a Slump test (IS 1199–1959). The slump cone was 20 cm in bottom diameter, 10 cm in top diameter and 30 cm in height. Concrete is poured in 4 layers; every layer is tamped 25 times with a tamping rod. As per IS 516–2004, various strength tests like compression, tension, flexural tests and durability tests such as water

absorption and sorptivity tests were conducted. Curing was achieved by keeping the specimens in water for controlled concrete, and for self-curing concrete, ambient curing was done.

3.1 Compression strength

The test was carried out by casting cubes of size 150 mm ×150 mm ×150 mm; concrete is filled in 3 layers, and each layer is given with 25 blows. After 24 h, the specimen is removed from the mould and kept for curing. After reaching the cure phase, the specimen is tested in a compressive testing machine. The load is applied till the specimen fails, at which point the maximum load is measured. The formula to determine the compressive strength is given by

$$\text{Compressive Strength} = \frac{\text{P}}{\text{A}}(\text{N/mm2}) \tag{7}$$

where: P = Compression load in kN.
A = C/S area of cube in mm.^{2}

3.2 Split tensile strength

Cylinders of dimensions 150 mm × 300 mm were cast to conduct the test. After the curing period, the specimen is tested in a compression machine by placing it horizontally, and the load is applied. The maximum load when the specimen fails is noted. The formula utilized in finding split tensile strength is given by

$$\text{Split tensile strength} = \frac{2\text{P}}{\pi\text{DL}}(\text{N/mm2}) \tag{8}$$

where: P = load in kN.
D = Dia of cylindrical specimen in mm.
L = Length of cylindrical specimen in mm.

3.3 Flexural strength

A flexural test was performed on a beam of size 150 mm × 150 mm × 700 mm using a two-point load machine. The load is applied at a constant rate until the specimen breaks and the maximum load is noted. The formula obtains the flexural strength.

$$\text{Flexural strength} = \frac{PL}{bd^2}(\text{N/mm2}) \tag{9}$$

where: P = Load in KN.
L = Length of beam in mm.
b = Breadth of the beam in mm.
d = Depth of beam in mm.

3.4 Water absorption test

Tests were done using cubes having dimensions of 150 × 150 × 150 mm. Specimens are dried to a consistent mass in an oven at 105 C. After that, weight is to be noted. The specimen is immersed in water when it has cooled to room temperature. The specimens were taken out from the water and weighed at regular intervals. The procedure is repeated until a consistent weight (Saturated completely) is obtained. The saturated water absorption is calculated. The absorption of saturated water is computed as follows:

$$\text{Water Absorption} = \frac{\text{W}_2 - \text{W}_1}{\text{W}_1} \times 100 \tag{10}$$

where: W_1 = oven-dried weight of specimen.
W_2 = completely saturated specimen weight.

3.5 Sorptivity test

Sorptivity refers to the capillary forces exerted by the pore structure, which cause fluids to be absorbed into the material's body. To determine the sorptivity of concrete, 150 × 150 × 150 mm dimensions cubes are to be cast and cured for 28 days. These cubes are pre-conditioned in the oven at 105 °C for 24 h and cooled for 24 h to attain a constant moisture level. To avoid evaporation and ensure uniaxial water flow during the test, four sides of the concrete specimen are sealed with paraffin wax or silicon sealant. At the same time, two opposing faces are left unsealed. The original weights of the specimens were recorded before they were placed in water. Only the specimen's lower 2 to 5 mm face is submerged in water. Water absorption is measured at predetermined intervals until the mass does not increase anymore. The following expression will be utilized to calculate the sorptivity coefficient.

$$S = \frac{Q/A}{\sqrt{t}} \tag{11}$$

Where: S = Sorptivity in mm/√min.
Q = volume of water absorbed in mm.
A = Surface area in contact with water in mm^2
t = time in min.

3.6 SEM

Scanning electron microscope [Carl Zeiss and Sigma (FESEM) with Gemini column] was used to examine the normal and internal curing concrete hydration products morphology and microstructure at an accelerating voltage to capture c and si lines at 20.00 kV. X-rays penetrated the samples to a depth of around 15 mm. Samples were placed on aluminum stubs with carbon tape, paste & gold coated in a sputtering machine to induce conductivity. After that, the coated samples were kept inside the scanning electron microscope.

3.7 Artificial neural network

The network structure determines the number of layers in a neural network and their roles. In most networks, there is an input, hidden, and output layers [59].

- Input layer: Every network has a layer of input neurons whose role is to feed information to the next layer of neurons. The number of design variables equals the number of neurons in the input layer.
- Hidden layer: These are the layers that exist between the i/p and o/p layers. These processing units must be used internally to connect the i/p and o/p units. These were also referred to as weighted connections.
- Output layer: The output of a neuron in a network is a weighted sum of its input, but a threshold function is also utilized to find the final value.

3.8 Feed-forward back propagation network (FFBPN)

- It is a widely adopted neural network model. Although there was no feedback connection, errors were propagated backward during training. Many applications can be developed utilizing an FFBPN using the least mean square error.
- Errors in the output determine measures of hidden layer output errors, which are the basis for adjusting the connection weights between the input and hidden layers.
- Adjusting the 2 sets of weights between the layers and collecting the outputs in an iterative process until the error is below a tolerance level.

3.9 Backpropagation training algorithm

1. The input and output vectors are applied to the network.
2. Calculate the network's output.
3. Calculate the error between the required o/p and the network o/p.

Table 1 Slump values of concrete

Grade	Slump values in mm
M40 (control mix)	100
M40-PEG 0.5%	102
M40-PEG 1%	102
M40-PEG 1.5%	103
M40-PEG 2%	104

Fig. 3 Experimental compressive strength values

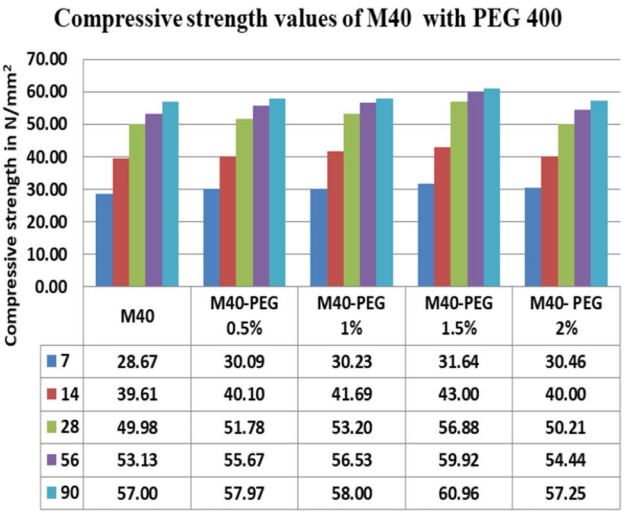

4. Minimize the error by adjusting the weights of the network.

Steps 1 through 4 should be repeated for each vector in the training set until the overall error is acceptable. The signal propagates from the network input to its outputs in steps one and two. This is referred to as a forward pass. Steps three and four are reverse passes, in which the estimated error signal is sent across the network and utilized to change weights.

4 Results and discussion

4.1 Fresh concrete properties

Workability is studied by conducting a slump test. Workability is the ease with which concrete is mixed, placed, consolidated, and finished by maintaining homogeneity. The slump values for M40 concrete are represented in Table 1.

4.2 Strength properties

Strength properties are determined by conducting compression, split tensile, and flexural tests by casting cubes, cylinders, and beams. After casting, all the specimens were cured for 7,14,28,56 and 90 days. The compressive, split tensile, and flexure strength of internally cured concrete is greater when compared with traditional concrete. In M40 concrete, 1.5% of self-curing agent strength obtained was maximum; for other percentages, strength decreased, as represented in Figs. 3, 4, and 5.PEG 400 is highly viscousy liquid it binds the concrete materials very firmly, after 1.5% of PEG400 mixing of concrete is very difficult.

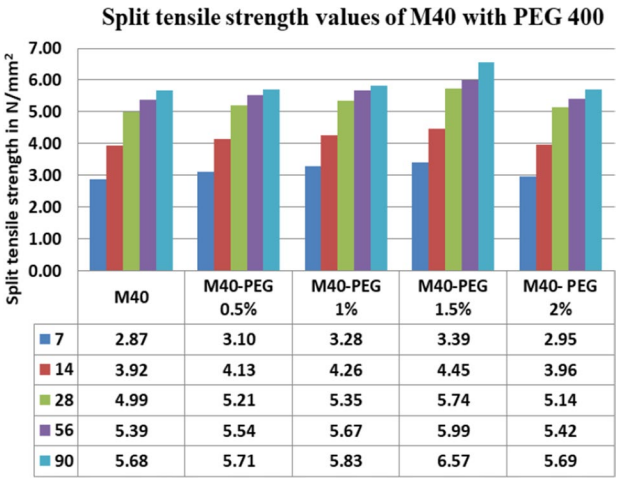

	M40	M40-PEG 0.5%	M40-PEG 1%	M40-PEG 1.5%	M40- PEG 2%
7	2.87	3.10	3.28	3.39	2.95
14	3.92	4.13	4.26	4.45	3.96
28	4.99	5.21	5.35	5.74	5.14
56	5.39	5.54	5.67	5.99	5.42
90	5.68	5.71	5.83	6.57	5.69

Fig. 4 Experimental split tensile strength values

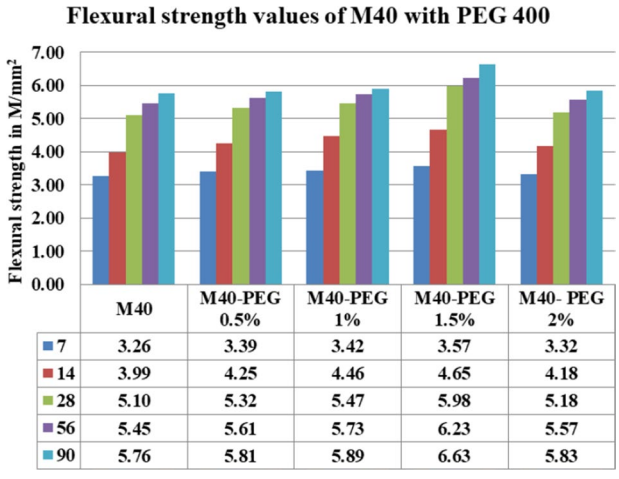

	M40	M40-PEG 0.5%	M40-PEG 1%	M40-PEG 1.5%	M40- PEG 2%
7	3.26	3.39	3.42	3.57	3.32
14	3.99	4.25	4.46	4.65	4.18
28	5.10	5.32	5.47	5.98	5.18
56	5.45	5.61	5.73	6.23	5.57
90	5.76	5.81	5.89	6.63	5.83

Fig. 5 Experimental Flexural Strength Values

Table 2 Water absorption values of M40 concrete

Grade	Water absorbtion (%)
M40	3.35
M40- PEG 0.5%	2.72
M40-PEG 1%	2.48
M40-PEG 1.5%	2.16
M40-PEG 2%	2.44

4.3 Water absorption

Water absorption was higher in normal concrete compared to internal curing concrete. Water absorption is less for M40-PEG 1.5%, as given in Table 2.

Table 3 Sorptivity val ues of concrete

Grade	Sorptivity value in 10^{-3} mm/min$^{0.5}$
M40	0.30
M40- PEG 0.5%	0.23
M40-PEG 1%	0.21
M40-PEG 1.5%	0.11
M40-PEG 2%	0.20

4.4 Sorptivity

Sorptivity was higher in normal concrete compared to internal curing concrete. The sorptivity value was minimum for M40-PEG 1.5%. The sorptivity graph is given in Table 3.

4.5 Validation of experimental results using ANN

The internal curing concrete predictive models were established using MATLAB ANN, and the created models were compared by regression analysis. A forward-back propagation algorithm was adopted. ANN model created consists of 9 input layers (cement, fly ash, water, w/c ratio, superplasticizer, PEG 400, coarse aggregate, fine aggregate, age), 1 hidden layer and 1 output layer (Strength). 70% of samples were considered for training, and 15% were taken for validation and testing. Regression coefficient values for the training, validation, testing, and overall are 0.98261, 0.98686, 0.98749, and 0.98368, respectively, for compressive strength is represented in Fig. 6.

Regression coefficient values for the training, validation, testing and overall are 0.99527, 0.99684, 0.99565 and 0.9953, respectively, for tensile strength is shown in Fig. 7.

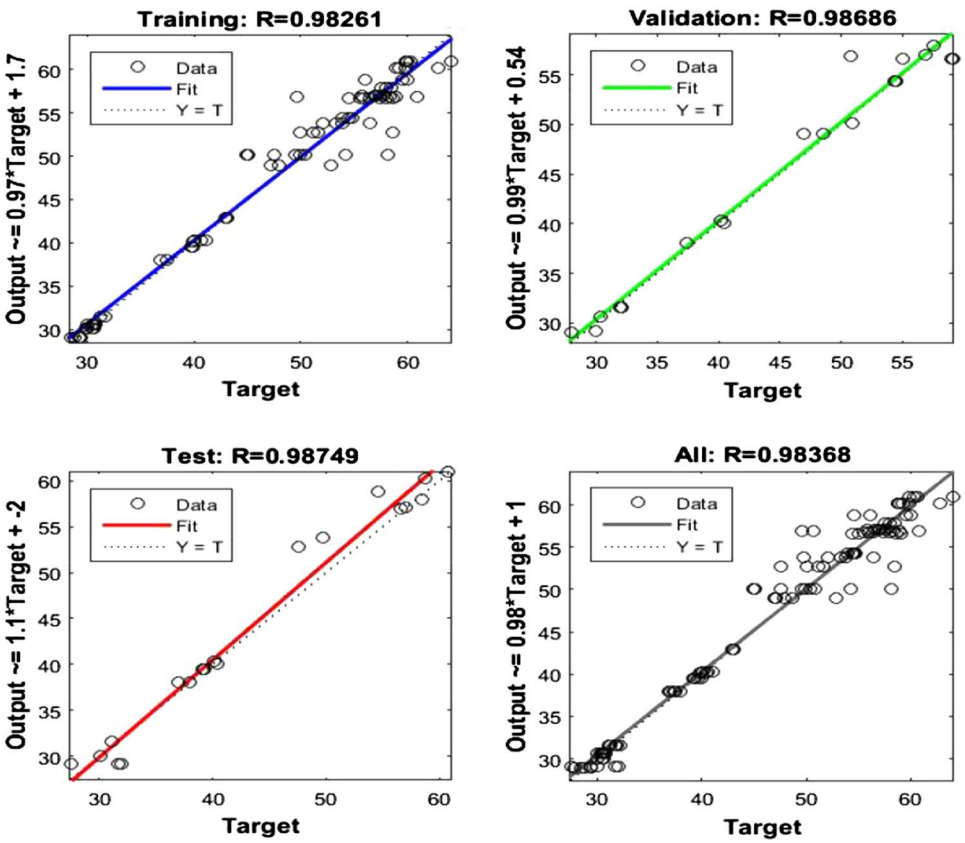

Fig. 6 Compressive strength plot of experiment v/s Predicted values

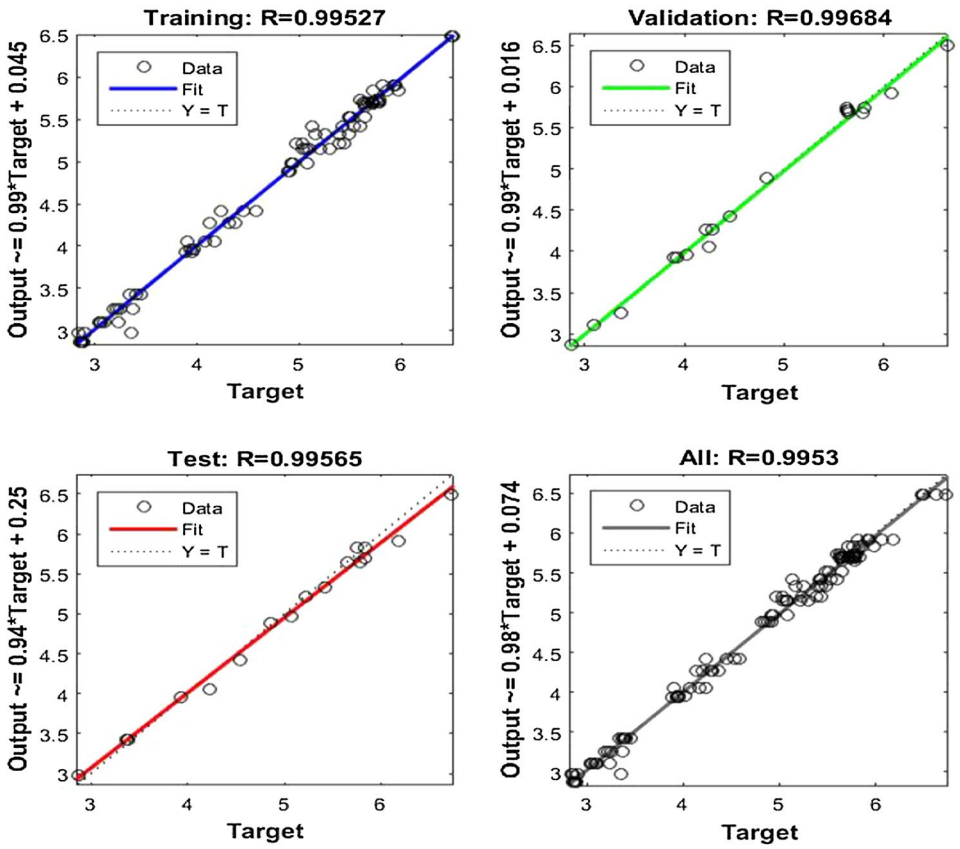

Fig. 7 Tensile strength plot of experiment v/s Predicted values

Regression coefficient values for the training, validation, testing, and overall are 0.98261, 0.98686, 0.98749, and 0.98368, respectively, for flexural strength, represented in Fig. 8.

4.6 Microstructural analysis

The analysis is carried out by scanning electron microscope graph shown in Figs. 9, 10, which reveals that normal concrete pores are more than internal curing concrete. CSH gel formation is excess in internal curing concrete; hence, it is stronger.

From the XRD spectra as shoen in Fig. 11 it is clear that M40 in addition of PEG was clearly indicated, thus results in the bond formation between them. In this scenario, the enhanced formation of the superlative C–S–H gel due to improvements is evident through prominent peaks corresponding to mineralogical components like Ca, Si, Al, and Fe. Conversely, the troughs in some mineralogical fractions are inevitable, likely stemming from variations in curing processes influenced by fluctuating gradients during the curing process—either normal or reverse—contingent upon the efficiency of the porous catalyst medium introduced. The crystallite size of the samples was calculated from Scherrer formula as shown in Table 4 for the obtained samples which depicts as the crystallite size varies with variation in the sample mixture.

5 Implications

This study has far-reaching implications. Using PEG-400 as an interior curing agent in concrete can transform building practices by allowing for more resource-efficient and ecologically conscientious procedures. Concrete's greater strength and durability and reduced water absorption boost the lifetime and resilience of concrete structures. The discoveries also contribute to the continuous search for novel solutions to building water shortage, making the technology applicable to various applications, from infrastructure initiatives to architectural endeavors.

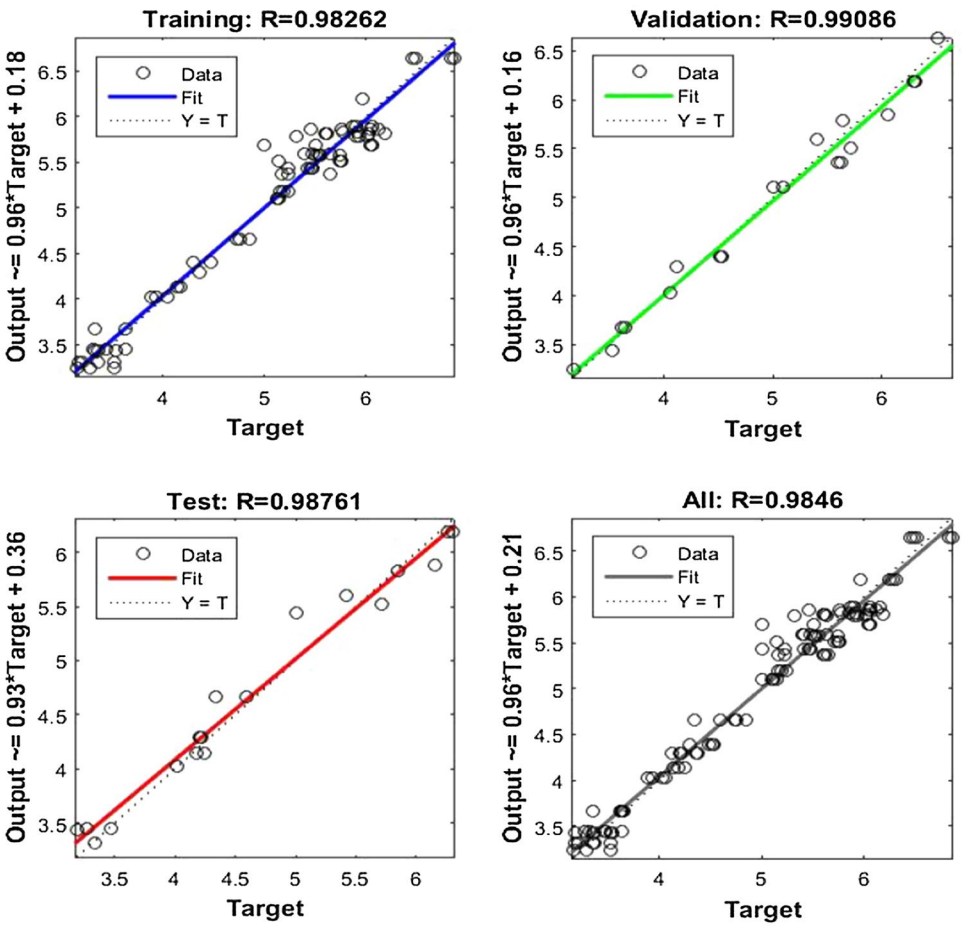

Fig. 8 Flexural strength plot of experiment v/s Predicted values

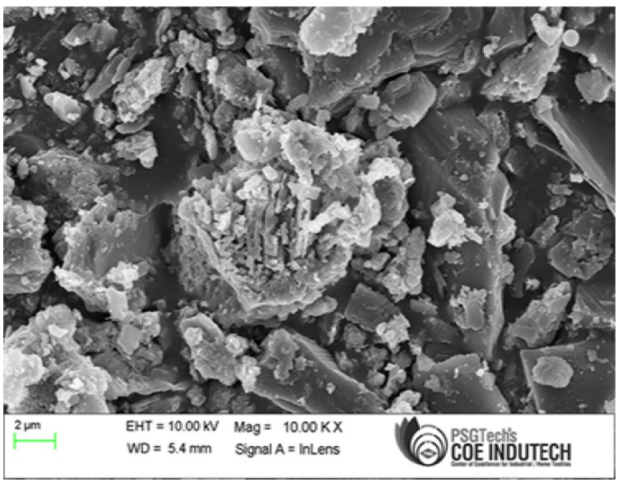

Fig. 9 SEM photomicrograph of M40 normal concrete after 28 days

6 Conclusions

This paper, PEG-400 is utilized as the internal curing agent in varying percentages to create internal curing concrete, and its effect on strength and durability properties has been studied. ANN has been implemented to compare the experimental findings. The following conclusions are drawn.

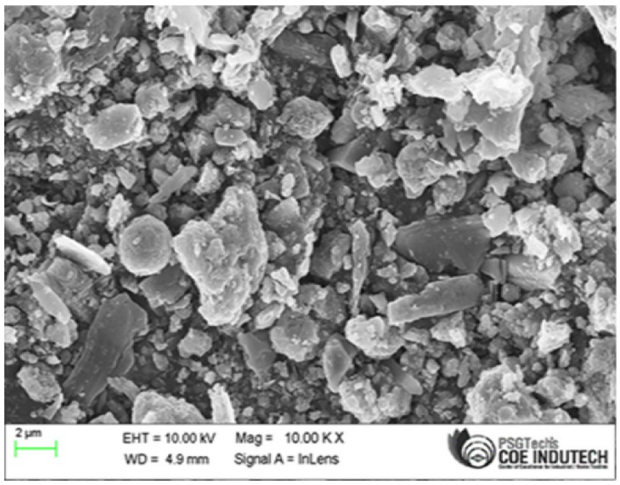

Fig. 10 SEM photomicrograph of M40- PEG 1.5% concrete after 28 days

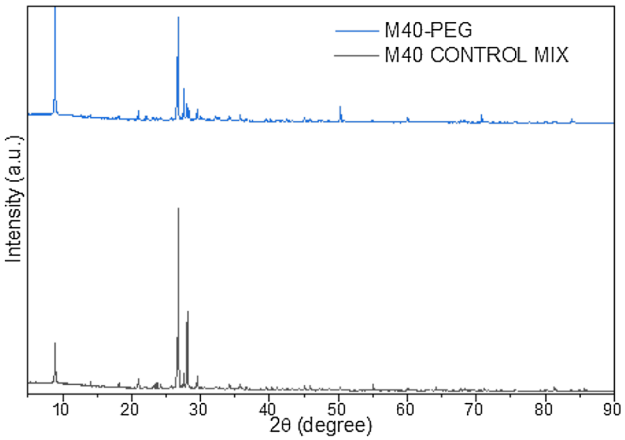

Fig. 11 XRD patterns of M40 control mix and M40-1.5%PEG

Table 4 crystallite size of normal and self curing concrete

Sample Code	Crystallite size (nm)
M40–control mix	53.029
M40–PEG	49.885

- The addition of PEG-400 in concrete results in self-curing, which retains water and inhibits surface evaporation. Internal curing concrete at 1.5% of PEG-400 obtained 13.81%, 15.03% and 17.25% increased compression, split tension and flexure strength, respectively, compared with conventional concrete.
- Water absorption and Sorptivity values are less in M40 internal curing concrete with 1.5% of PEG 400 than normal concrete and other percentage variations of PEG 400 in internal curing concrete.
- The microstructure of internal curing concrete indicates that the pore sizes are small compared to conventional concrete due to the presence of hydrogen bonds.
- X-ray diffraction (XRD) analysis has revealed that the crystallite size is more in conventional concrete mix when compared to internal curing concrete. Smaller crystallites typically have a larger surface area compared to larger crystallites. This increased surface area allows for more rapid interaction between cement particles and water. As a result, the hydration process tends to accelerate in concrete with small crystallites.
- The ANN-predicted results are much closer to the experiment values.

7 Limitations

While the study provides encouraging insights, there are numerous constraints to consider. The scope of the study may not include all conceivable differences in concrete mixes, curing conditions, and real-world circumstances. The findings are based on specific settings, and the efficiency of the recommended approach may vary depending on the situation. Furthermore, the research may not cover all potential problems or unforeseen consequences of widespread adoption.

8 Future directions

The study opens the door to more inquiry and investigation. Future research might optimize the PEG-400 concentration and investigate its compatibility with various cement and concrete combinations. Long-term studies are required to evaluate the durability and performance of PEG-400-treated concrete under various environmental conditions. Comparative research with various internal curative agents and approaches may offer a more complete picture of the benefits. Furthermore, predictive models such as ANN might be broadened to include larger datasets, improving accuracy and predictive capabilities.

Author contributions 1. SGV and NCKN Wrote the Main Paper 2. SBA - Analysis 3. TM - Software and review 4. BA, EAF- Technical laboratory support.

Data availability Data will be made available on request.

Declarations

Competing interests The authors declare no competing interests.

References

1. Mohammed Shafeeque V, Sanofar PB, Praveen KP. Strength comparison of self-curing concrete and normal curing concrete. SSRG Int J vil Eng. 2016;3(3):47–52.
2. Basil Joseph M 2016. Studies on properties of self-curing concrete using poly-ethylene glycol. IOSR Journal of Mechanical and Civil Engineering. 12–17.
3. Venkata Reddy N, Anvesh Reddy IS. Study on self curing concrete using liquid paraffin wax as external agent. Int J Eng Res General Sci. 2016;4(6):29–34.
4. Mandiwal P, Jamle S. Tensile strength & durability study on self-curing concrete as a partial replacement of cement by PEG-400. Int J Res Eng Appl Manag. 2019;04(10):244–8.
5. Subrahmanya R, Kumar P, Naresh Kumar T, Narayana SMV. A study on strength comparison of self-curing concrete with replacement of fly ash. Int J Sci Res Sci Technol. 2018;4(2):305–14.
6. Randhawa KS, Chauhan R, Kumar R. An investigation on the effect of lime addition on UCS of Indian black cotton soil. Mater Today Proc. 2022;50:797–803.
7. Zhen Li, Jiaping L, Jianzhuang X, Peihua Z. Internal curing effect of saturated recycled fine aggregates in early-aged mortor. Cement Concrete Composite. 2019;108:10344.
8. Kumar R, Banga HK, Singh H, Kundal S. An outline on modern day applications of solid lubricants. Mater Today Proc. 2020;28:1962–7.
9. Remya KM, Shilpa VS. Experimental study on strength characteristics of self curing concrete using poly ethylene glycol and lightweight aggregate. Int J Res Adv Special Issue Int Conf Technol Adv Struct Constr. 2015;10–11:73–7.
10. Vishnu T, Beena BR. An experimental investigation of self-curing concrete incorporated with light weight fine aggregate and polyethylene glycol. Int J Innov Res Sci Technol. 2016;3(04):116–22.
11. Darshni P, Dhaliwal BS, Kumar R, Balogun VA, Singh S, Pruncu CI. Artificial neural network based character recognition using SciLab. Multimed Tools Appl. 2023;82(2):2517–38.
12. Chand MSR, Giri PSNR, Kumar PR, Kumar GR, Raveena C. Effect of self curing chemicals in self compactiong mortar. Constr Build Mater. 2016;107:356–64.

13. Goyal LK, Chauhan R, Kumar R, Rai HS. Use of BIM in development of smart cities: a review IOP conference series: materials science and engineering. Bristol: IOP Publishing; 2020.
14. Gaston E-H, Lopez M. Extending internal curing to concrete mixtures with w/c higher than 0.42. Constr Build Mater. 2011;25:1236–42.
15. Mousa MI, Mahdy MG, Abdel-Reheem AH, Yehia AZ. Self-curing concrete types; water retention and durability. Alex Eng J. 2015;54(3):565–75.
16. Akhib K, Kumar V. A study on mechanical properties of self-curing M65 grade concrete by using polyethylene glycol. Int J Eng Sci Comput. 2018;8(5):17543–6.
17. Kim HK, Lee HK. Hydration kinetics of high-strength concrete with untreated coal bottom ash for internal curing. Cement Concrete Composite. 2018;91:67–75.
18. Mandiwal P, Jamle S. Use of polyethylene glycol as self curing agent in self curing concrete—an experimental approach. Int Res J Eng Technol. 2018;05(11):916–8.
19. Sebastin S, Franchis David M. Study on mechanical properties of self-curing concrete with partial replacement of granite powder as fine aggregate. J Ceramics Concrete Technol. 2021;6(1):38–54.
20. Gopala Krishna Sastry KVS, Kumar PM. Self-curing concrete with different self-curing agents. Mater Sci Eng. 2018;330: 012120.
21. Peihua Z, Mateusz W, Nikolajs T, Lei Li, Jiaping L, Pietro L. Internal curing with superabsorbent polymers of different chemical structures. Cem Concr Res. 2019;123: 105789.
22. Xiao Q, Aiqin S, Henghua L, Liwan S, Jingyu Y, Huifen L. Research on water transport behaviors and hdration characteristics of internal curing pavement concrete. Constr Build Mater. 2020;248: 118714.
23. El-Hawary M, Al-Sulily A. Internal curing of recycled aggregates concrete. J Clean Prod. 2020;27: 122911.
24. Mohammad B, Weijin Z, Garboczi EJ, Oo NY, Sabrina S, Hsuan GY, Pieter B, Yaghoob F. Potential use of lightweight aggregate (LWA) produced from bottom coal ash for internal curing of concrete systems. Cement Concrete Composite. 2020;105: 103428.
25. Mateusz W, Alexander A, Christoph H, Pietro L. Microstructure development and autogenous shrinkage of mortars with C-S-H seeding and internal curing. Cem Concr Res. 2020;129: 105967.
26. Al DM, Saffar AJK, Saad A, Tayeh BA. Effect of internal curing on behavior of high performance concrete: an overview case studies in construction. Case Stud Constr Mater Mater. 2019. https://doi.org/10.1016/j.cscm.2019.e00229.
27. Shivaprasad SR, Maneeth S, Brijbhusan PD, Siddharath S. To evaluate strength properties of fibre reinforced concrete with additives using different curing agents. Int J Computat Eng Res. 2018;08(6):2250–3005.
28. Yuan X, Peng X, Yi L, Yong X. Experimental study of self-curing concrete. Eng Sci Technol J. 2020;2(1):1–19.
29. Sabaoon AM, Singh N. Experimental investigation of self-curing concrete by using natural and chemical admixtures Indian. J Sci Technol. 2019;12(5):1–6.
30. Nehdi M, El Chabib H, El Naggar MH. Predicting performance of self-compacting concrete mixtures using artificial neural networks. Materials Journal. 2016;98(5):394–401.
31. Saha P, Prasad MLV, Kumar PR. Predicting strength of scc using artificial neural network and multivariable regression analysis. Comput Concr. 2017;20(1):31–8.
32. Reddy TCS. Predicting the strength properties of slurry infiltrated fibrous concrete using artificial neural network. Front Struct Civ Eng. 2018;12(4):490–503.
33. Bui DK, Nguyen T, Chou JS, Nguyen-Xuan H, Ngo TD. A modified firefly algorithm-artificial neural network expert system for predicting compressive and tensile strength of high-performance concrete. Constr Build Mater. 2018;180:320–33.
34. Awoyera PO. Predictive models for determination of compressive and split-tensile strengths of steel slag aggregate concrete. Mater Res Innovations. 2018;22(5):287–93.
35. Kaplan G, Yaprak H, Memiş S, Alnkaa A. Artificial neural network estimation of the effect of varying curing conditions and cement type on hardened concrete properties. Buildings. 2019;9(1):10.
36. Hunga PD, Sub NT, Diep VT. Surface classification of damaged concrete using deep convolutional neural network. Pattern Recognit Image Anal. 2019;29(4):676–87.
37. Uchechukwu E, Austin O. Artificial neural network application to the compressive strength of palm kernel shell concrete. MedCrave Online J Civil Eng. 2020;6(1):1–10.
38. Chandel RS, Kumar R, Kapoor J. Sustainability aspects of machining operations: a summary of concepts. Mater Today Proc. 2022;50:716–27.
39. Ranjan N, Kumar R, Kumar R, Kaur R, Singh S. Investigation of fused filament fabrication-based manufacturing of ABS-Al composite structures: prediction by machine learning and optimization. J Mater Eng Perform. 2023;32(10):4555–74.
40. Cusson D, Hoogeveen T. Internal curing of high-performance concrete with presoaked fine lightweight aggregate for prevention of autogenous shrinkage cracking. Cem Concr Res. 2018;38:757–65.
41. Thakur V, Kumar R, Kumar R, Singh R, Kumar V. Hybrid additive manufacturing of highly sustainable polylactic acid-carbon fiber-polylactic acid sandwiched composite structures: optimization and machine learning. J Thermopl Compos Mater. 2023;37:08927057231180186.
42. Mohanraj A, Manoj Prabhakar S, Rajendran M. Predicting the strength of self-compacting self-curing concrete using artificial neural network. Int J Civil Eng Technol. 2014;5(12):239–47.
43. Chithra S, Kumar SS, Chinnaraju K, Ashmita FA. A comparative study on the compressive strength prediction models for high performance concrete containing nano silica and copper slag using regression analysis and artificial neural networks. Constr Build Mater. 2016;114:528–35.
44. Khademi F, Jamal SM. Predicting the 28 days compressive strength of concrete using artificial neural network. J Civil Eng. 2016;6(2):1.
45. Wyrzykowski M, Assmann A, Hesse C. Microstructure development and autogenous shrinkage of mortars with C-SH seeding and internal curing. Cem Concr Res. 2020;129: 105967.
46. Yang S, Wang L. Effect of internal curing on characteristics of self-compacting concrete by using fine and coarse lightweight aggregates. J Mater Civil Eng. 2017;29(10):04017186.
47. Huseien GF, Judah ZH, Memon RP, Sam ARM. Compressive strength and microstructure properties of modified concrete incorporated effective microorganism and fly ash. Mater Today Proc. 2021;46:2036–44.

48. Huseien GF, Joudah ZH, Khalid NHA, Sam ARM, Tahir MM, Lim NHAS, Alyousef R, Mirza J. Durability performance of modified concrete incorporating fly ash and effective microorganism. Constr Build Mater. 2021;267: 120947.
49. Soler J M. Thermodynamic description of the solubility of CSH gels in hydrated Portland cement. Literature review. Posiva, Finland. 2007. 1–36.
50. Dhir RK, Hewlett PC, Lota JS, Dyer TD. An investigation into the feasibility of formulating self-cure concrete. Mater Struct. 1994;27:606–15.
51. Dhir RK, Hewlett PC, Dyer TD. Mechanisms of water retention in cement pastes containing a self-curing agent. Mag Concr Res. 1998;50:85–90.
52. Sastry KVSGK, Kumar PM. Self-curing concrete with different self-curing agents IOP conferences series. Mater Sci Eng. 2018;330:012120.
53. Chand MSR, Giri PSNR, Pancharathi RK, Kumar GR, Raveena C. Effect of self curing chemicals in self compactingmortars. Constr Build Mater. 2016;107:356–64.
54. Sarbapalli D, Dhabalia Y, Sarkar K, Bhattacharjee B. Application of SAP and PEG as curing agents for ordinary cementbased systems: Impact on the early age properties of paste and mortar with water-to-cement ratio of 0.4 and above. Eur J Environ Civil Eng. 2016;21:1237–52.
55. Chand MSR, Kumar PR, Giri PSNR, Kumar GR. Performance and microstructure characteristics of self-curing self-compacting concrete. Adv Cem Res. 2018;30:451–68.
56. El Wakkad N Y, Heiza H and Eladly A.Review on self-curing concrete. In 11th International Conference on Nano Technology in Construction. Sharm El-Sheikh, Egypt, 22–25 March 2019; pp. 1–16.
57. Alberty RA, Daniels F. Physical Chemestry. 5th ed. NY: John Wiley and Sons Ltd; 1975.
58. Kamal M, Safan M, Bashandy A, Khalil A. Experimental investigation on the behavior of normal strength and high strength self-curing self-compacting concrete. J Build Eng. 2018;16:79–93.
59. Goyal KK, Sharma N, Dev Gupta R, Singh G, Rani D, Banga HK, Kumar R, Pimenov DY, Giasin K. A soft computing-based analysis of cutting rate and recast layer thickness for AZ31 alloy on WEDM using RSM-MOPSO. Materials. 2022;15(2):635. https://doi.org/10.3390/ma15020635.